Int. J. Morphol.,
40(4):1000-1008, 2022.

A Comparative Study of the Morphology of Suboccipital Cavernous Sinus Using Magnetic Resonance Imaging and Cast Specimens

Un Estudio Comparativo de la Morfología del Seno Cavernoso Suboccipital Utilizando Imágenes de Resonancia Magnética y Muestras de Yeso

Si-Meng Jiang[1,4]; Cong Liu[2,4]; Xu-Hui Zhang[3,4]; Nan Zheng[3]; Sheng-BoYu[3]; Yan-Yan Chi[3]; Jian-Fei Zhang[3]; Ye Wang[2]; Hong-Jin Sui[3] & Qiang Xu[2]

JIANG, S. M.; LIU, C.; ZHANG, X. H.; ZHENG, N.; BOYU, S.; CHI, Y. Y.; ZHANG, J. F.; WANG, Y.; SUI, H. J. & XU, Q. A comparative study of the morphology of suboccipital cavernous sinus using magnetic resonance imaging and cast specimens. *Int. J. Morphol., 40(4)*:1000-1008, 2022.

SUMMARY: A comparative study of the morphology of suboccipital cavernous sinus (SCS) using MRI and cast specimens was performed. The present retrospective study analysed the craniocervical magnetic resonance venography (MRV) imaging data of 61 patients. Three-dimensional reconstruction was performed using Mimics 19.0. The SCS left-right diameter(d1), distance from the midline (d2), supero-inferior diameter(d3), anteroposterior diameter (d4), distance from posterior diameter to skin (d5), and diameter of the SCS at different parts (d6-d8) were measured. Comparison between MRV images and cast specimens, the SCS, marginal sinus, anterior condylar vein, and vertebral artery venous plexus were symmetrical and could be bilaterally displayed, whereas the presence of extra condylar vein and posterior condylar vein exhibited different types. The adjacency between the SCS and its communicating vessels and changes in its communicating vessels corresponded well with the MRV images and cast specimens. Many types of the presence of left and right lateral condylar and posterior condylar veins were found in the cast specimens, which could be divided into the bilateral presence of posterior condylar and lateral condylar veins, unilateral presence of posterior condylar veins, and unilateral presence of lateral condylar vein. A total of 61 cases analysed using MRV images revealed the bilateral presence of posterior condylar and lateral condylar veins (77.1 %), the unilateral presence of posterior condylar vein (18.0 %), and the unilateral presence of lateral condylar vein (9.8 %), of which the bilateral presence of posterior condylar and lateral condylar veins accounted for the largest proportion. MRV images and cast specimens of the SCS showed its normal morphological structure and adjacency, thus providing accurate and complete Three-dimensional imaging anatomical data of the SCS and its communicating vascular structures. This study enriches the Chinese SCS imaging anatomy data and may be valuable in clinical practice.

KEY WORDS: Suboccipital cavernous sinus; MRV; Cast specimen, Craniocervical junction.

INTRODUCTION

The craniocervical junction (CCJ) is an area surrounded by the lower edge of the occipital bone to the dentata. It consists of vital structures such as medulla oblongata, upper cervical spinal cord, cranial nerve, vertebral artery, and internal carotid artery and vein. Because of its complex anatomical structure, performing surgery in this area is associated with substantial risks. SCS, first reported in 1997 (Arnautovic *et al*., 1997), is a venous plexus structure that is located in the suboccipital region and surrounds the horizontal suboccipital segment (V3) of the vertebral artery and its branches, the periarterial autonomic plexus, and adjacent spinal nerves. SCS is similar to the intracranial cavernous sinus in terms of the anatomical structure, function, pathological features, and transitional patterns of the arterial wall of the perforating artery. MRV images display an irregular shape of the SCS, with a long strip or oval

[1] Postgraduate Training Base, The 967 Hospital of the Joint Logistics Support Force Jinzhou Medical University, Dalian 116021, China.
[2] Department of Radiology, The 967 Hospital of the Joint Logistics Support Force, Dalian 116021, China.
[3] Department of Anatomy, College of Basic Medicine Dalian Medical University, Dalian 116044, China.
[4] These authors contributed equally: Si-Meng Jiang; Cong Liu; Xu-Hui Zhang.
Received: 2022-04-17 Accepted: 2022-05-18

shape in the coronal and sagittal planes and an irregular sector shape in the transverse plane. Increasing studies on the SCS have indicated the pivotal physiological role of the SCS and its surrounding venous structures in cranial venous drainage and highlighted their importance in the diagnosis and treatment of infectious diseases, tumour dissemination, and dural arteriovenous fistulas in this region (Hiramatsu *et al*., 2015). Therefore, identifying the fine anatomical structure of the SCS in clinical practice, especially for the protection of blood vessels and the reduction of complications during craniocervical junction surgery, is of great significance. This study enriches the fine anatomical data of the Chinese SCS and presents morphological reference data for the clinical individualised surgical plan to ensure safety of the surgery.

MATERIAL AND METHOD

Approval for this study was obtained from the Ethics Committee for Research of Basic Medical College of Dalian Medical University.

General information. The imaging data of cranial MRV performed in the 967 Hospital of the Joint Logistics Support Force between April 2012 and December 2021 were retrospectively analysed, and a total of 61 patients (including 40 males and 21 females), aged 8-72 years, with the mean age of 39.3±18.2 years, were enrolled. Inclusion criteria: MRV images without artifacts.

Exclusion criteria: (1) significant stenosis of the suboccipital vertebral artery; (2) venous sinus or venous thrombosis in the SCS and communicating vessels.

Scanning equipment and method. MRV scanning parameters: A 1.5T GE magnetic resonance scanner was used, with TR 3.7 ms/TE 1.3 ms; flip angle of 25°; FOV of 240 mm×240 mm; matrix of 512×512; and level thickness of 2.4 mm. Following the injection of gadoterate meglumine (Gd-DOTA) at a dose of 0.1 mmol/kg, scanning was performed without intervals. All patients had signed informed consent before the study.

Mimics three-dimensional reconstruction: The Mimics 19.0 image post-processing workstation was used. First, the original image data were imported for post-processing, and then, the MRV coronal, sagittal, and cross-sectional images were reconstructed. The diameters of the SCS were measured using its own tools, and the display and changes in the SCS and its communicating vessels were observed under the three reconstruction levels.

Study content

1.Three-dimensional reconstruction of MRV images and measurement of SCS diameters.

- Measurement of the SCS coronal left-right diameter (d1), distance from the midline (d2), and supero-inferior diameter (d3). Level selection: the most clearly displayed level of the SCS was measured; for d3, three points were measured, and their mean was calculated. There three points were: the exit of the vertebral artery from the foramen transversarium; the entrance of the vertebral artery into the dura mater; and the midpoint of the aforementioned two points.

- Measurement of the SCS sagittal anteroposterior diameter (d4) and the distance from the posterior diameter to the skin (d5). Level selection: the venous plexus surrounding its structure was measured at the level of the horizontal segment (V3) of the vertebral artery.

- Measurement of the transverse diameter of the initial part (d6), middle part (d7), and terminal part (d8) of SCS. Level selection: the initial part was the exit of the vertebral artery from the foramen transversarium; because of the lack of landmarks, the middle part was considered the midpoint of the initial part and the terminal part in the coronal plane. The terminal part was the entrance of the vertebral artery into the dura mater. The measurement plane was perpendicular to the vertebral artery.

2. Observations and display of the adjacency between SCS and its communicating vessels (marginal sinus, anterior condylar vein, posterior condylar vein, lateral condylar vein, and vertebral artery venous plexus) and variations in these communicating vessels.

Cast specimens

Materials. Six fresh non-traumatic head and neck specimens were obtained from the Department of Anatomy, College of Basic Medicine Dalian Medical University. Perfusate materials were: xylene, silica gel, 1.5 %-5 % curing agent, red and blue oil painting pigments (red for arteries and blue for veins), and warm normal saline.

Methods. Perfusate preparation: To prepare the perfusate, xylene and silica gel were mixed in a 1:1 ratio, to which 2.5 % curing agent was added. Subsequently, red and blue oil painting pigments were added to the mixture separately to the perfusate in a 15:1 ratio for distinguishing between arteries and veins.

Perfusion process: Common carotid artery, vertebral artery, and internal jugular vein were catheterised and washed with

approximately 500 mL of warm normal saline. The perfusate was injected into the common carotid artery, vertebral artery, and internal jugular vein on one side in turn, with approximately 60 mL of total arterial perfusion and 80 mL of venous perfusion. When perfusate exudation was observed in the common carotid artery, vertebral artery, and internal jugular vein on the other side and resistance in pushing the syringe, the filling of head and neck vascular perfusate was performed.

Corrosion and treatment: After approximately 48h and complete solidification of the casting filler, the specimens were immersed in concentrated hydrochloric acid solution in the upright position for corrosion to ensure that the position of each structure does not change during the preparation of casting specimens. The specimens were then taken out and rinsed after 2 weeks and trimmed as appropriate. Thereafter, the adjacency of the SCS and its communicating vessels and changes in its communicating vessels were observed on these cast specimens.

Statistical analysis. The measured data were analysed using SPSS 26.0 statistical software, and the results are expressed as the mean±standard deviation (X±S). The SCS left-right diameter values were compared using a paired sample T-test and the transverse diameters of the initial, middle, and terminal parts of the SCS were compared using One-Way ANOVA analysis. A p value of less than 0.05 indicated a statistically significant difference.

RESULTS

Coronal diameter of the SCS. The coronal measurement indicators of the SCS included d1, d2, and d3 (Fig. 1A). The measurement results are shown in Table I. Analysis of the measurements using the paired sample T-test showed no significant difference between the left and right sides (P>0.05).

Sagittal diameter of the SCS. The sagittal measurement indicators of the SCS included d4 and d5 (Fig. 1B). The measurement results are shown in Table II. Analysis of the measurements using the paired sample T-test indicated no significant difference between left and right sides (P>0.05).

Transverse diameter of the SCS. The transverse measurement indicators of the SCS included d6, d7, and d8. The initial part was the exit of the vertebral artery from the transverse foramen. The middle part was considered the midpoint of the initial part and the terminal part on the coronal plane because of the lack of landmarks. The terminal part was the entrance of the vertebral artery into the dura mater, which should be perpendicular to the vertebral artery as far as possible during the measurement (Fig. 1C-E). The measurement results are shown in Table III. Analysis of the measurements using the paired sample T-test displayed no significant difference between the left and right sides (P > 0.05); One-Way ANOVA analysis of variance showed a statistically significant difference between d6, d7, and d8 of the SCS (P<0.05) (Table IV), with the thinnest diameter in the initial part and the thickest diameter in the middle part.

SCS and communicating vessels in MRV images.

1. Observations of SCS adjacency to its communicating vessels in MRV images. The SCS, marginal sinus, vertebral artery venous plexus, anterior condylar vein, posterior condylar vein, and lateral condylar vein were completely

Table I. Comparison of SCS Coronal Measurements between Left and Right (unit: mm).

Item		Mean ± SD	T value	P value
Left-right diameter (d1)	Right	20.49 ± 0.93	- 0.414	0.680
	Left	20.52 ± 1.29		
Distance from the midline (d2)	Right	11.40 ± 0.98	1.470	0.147
	Left	11.21 ± 1.06		
Supero-inferior diameter (d3)	Right	7.11 ± 0.46	- 0.999	0.322
	Left	7.13 ± 0.55		

Note: P<0.05 in the paired sample T-test indicate a significant difference.

Table II. Comparison of SCS Sagittal Measurements between Left and Right (unit: mm).

Item		Mean ± SD	T value	P value
Antero-posterior diameter (d4)	Right	12.94 ± 0.71	1.145	0.257
	Left	12.85 ± 0.53		
Distance from the posterior	Right	39.21 ± 1.90	-0.580	0.564
diameter	Left	39.31 ± 2.09		

Note: P <0.05 in the paired sample T-test indicate a significant difference.

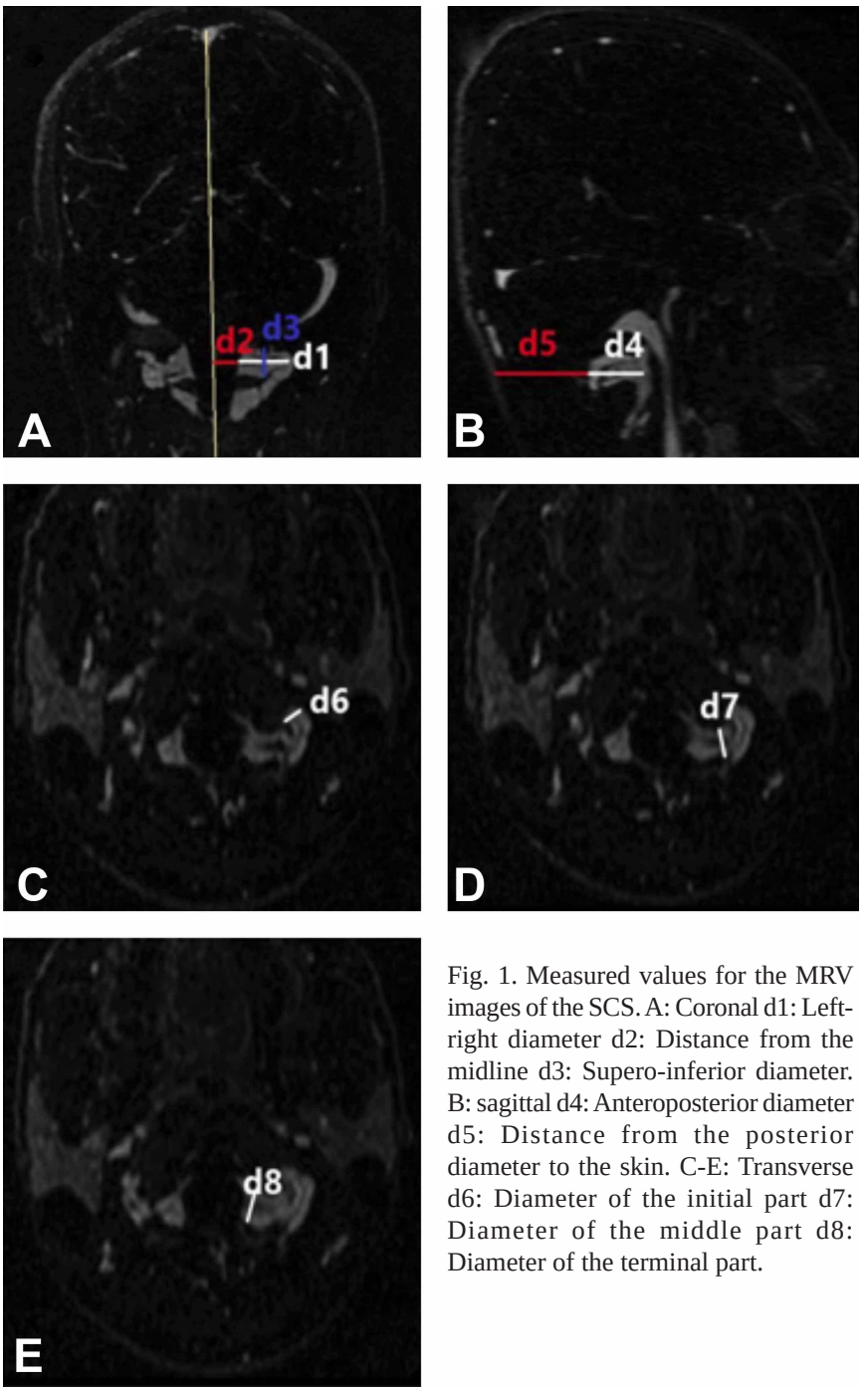

Fig. 1. Measured values for the MRV images of the SCS. A: Coronal d1: Left-right diameter d2: Distance from the midline d3: Supero-inferior diameter. B: sagittal d4: Anteroposterior diameter d5: Distance from the posterior diameter to the skin. C-E: Transverse d6: Diameter of the initial part d7: Diameter of the middle part d8: Diameter of the terminal part.

seen in the MRV images (Fig. 2). The SCS was connected to: the anterior condylar vein through its superomedial aspect (Figs. 2B and D); the lateral condylar vein through its anterolateral aspect (Fig. 2A); and the jugular bulb through the posterior condylar vein (Figs. 2B and D). It extended inferiorly to the vertebral artery venous plexus (Figs. 2B and D).

2. Observations and comparison of 61 cases of three-dimensional reconstructed cranial MRV images with those of cast specimens. The SCS, marginal sinus, vertebral artery venous plexus, and anterior condylar vein can be completely seen in the MRV images. However, the posterior condylar vein and lateral condylar vein can be displayed unilaterally or bilaterally, which led to the following difference in the MRV images: the bilateral display was called the bilateral presence of posterior condylar and lateral condylar veins (77.1 %), whereas the unilateral display was called the unilateral presence of posterior condylar vein (18.0 %) and the unilateral presence of lateral condylar vein (9.8 %). The bilateral presence of posterior condylar and the lateral condylar veins accounted for the largest proportion.

Observations of the cast specimens showed that the SCS, anterior condylar vein, and vertebral artery venous plexus can be bilaterally displayed, whereas the posterior condylar vein and lateral condylar vein can be unilaterally or bilaterally displayed, which led to the following difference in the cast specimens: the

Table III. Comparison of SCS Transverse Measurements between Left and Right (unit: mm).

Item		Mean ± SD	T value	P value
Diameter of the initial part(d6)	Right	8.20 ± 0.36	0.769	0.445
	Left	8.17 ± 0.33		
Diameter of the middle part(d7)	Right	10.68 ± 0.48	- 0.627	0.533
	Left	10.71 ± 0.57		
Diameter of the terminal part(d8)	Right	9.14 ± 0.54	0.601	0.550
	Left	9.12 ± 0.57		

Note: P<0.05 in the paired sample T-test indicate a significant difference.

bilateral display was called the bilateral presence of posterior condylar and lateral condylar veins, whereas the unilateral display was called the unilateral presence of posterior condylar vein and the unilateral presence of lateral condylar vein. This observation is consistent with the observations of the SCS MRV images. We selected cast

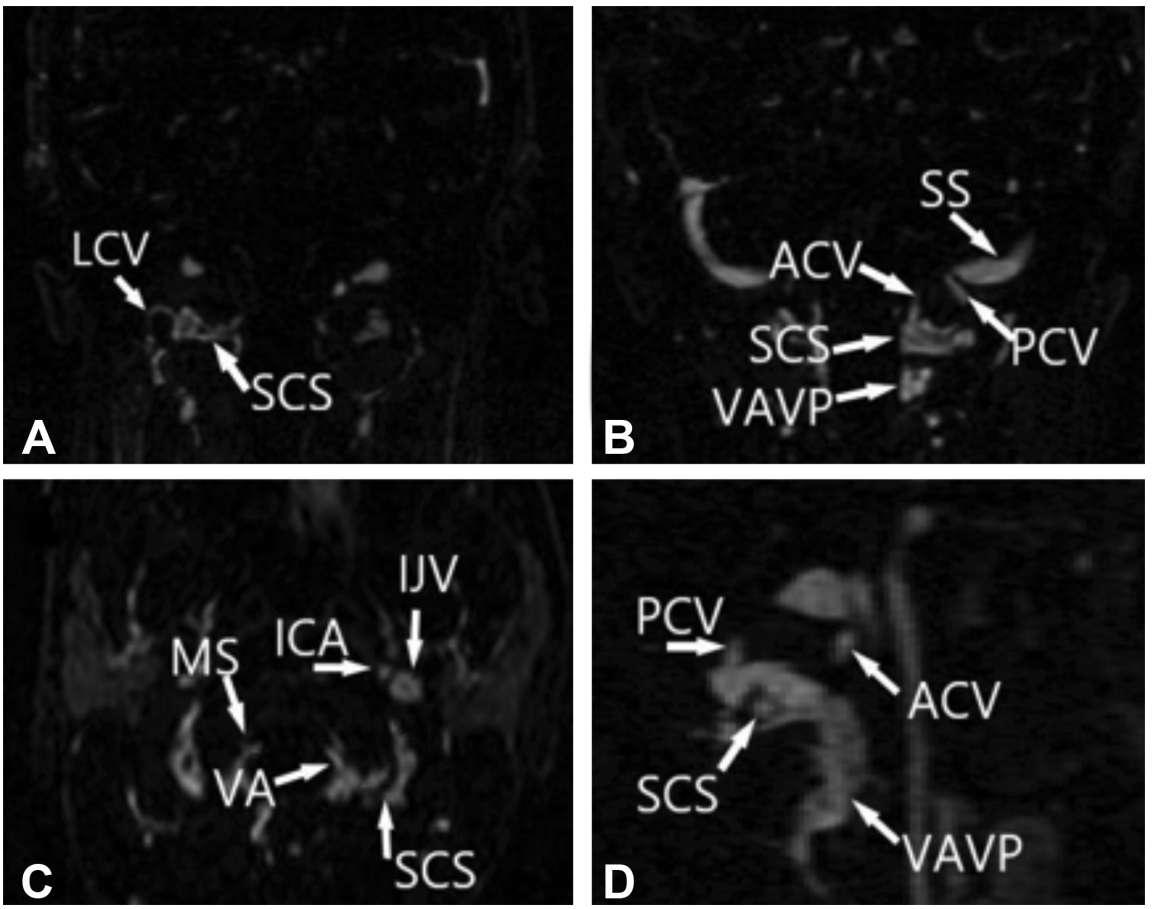

Fig. 2. Suboccipital cavernous sinus (SCS) magnetic resonance venography (MRV) images. A (coronal view): The SCS communicates with the lateral condylar vein through its anterolateral aspect. Fig.B (coronal view): The SCS communicates with the anterior condylar vein through its superomedial aspect and the posterior condylar vein through its superolateral aspect. It extends inferiorly to the vertebral artery venous plexus. Fig. C (transverse view): The irregular shape of SCS. The marginal sinus, vertebral artery, internal jugular vein, and internal carotid artery are seen in the transverse plane. Fig. D (sagittal view): The SCS communicates with the anterior condylar vein through its superomedial aspect and with the posterior condylar vein through its superolateral aspect. It extended inferiorly to the vertebral artery venous plexus. SCS: suboccipital cavernous sinus. ACV: anterior condylar vein; VAVP.Vertebral arterial venous plexus. PCV. posterior condylar vein. LCV. lateral condylar vein. IVJ: internal jugular vein; VA:vertebral artery; MS:marginal sinus; ICA:Internal carotid artery.

Table IV. Correlation Analysis of SCS Transverse Measurements in Each Group (unit: mm)

Item		Mean 95% confidence interval	P value
Diameter of the initial part	Right	8.11-8.29	
	Left	8.09-8.25	
Diameter of the middle part	Right	10.56-10.80	
	Left	10.57-10.86	
Diameter of the terminal part	Right	9.00-9.28	
	Left	8.97-9.27	
Group comparison	Right		0.00
	Left		0.00

Note: P<0.05 in One-Way ANOVA analysis of variance indicate a significant difference.

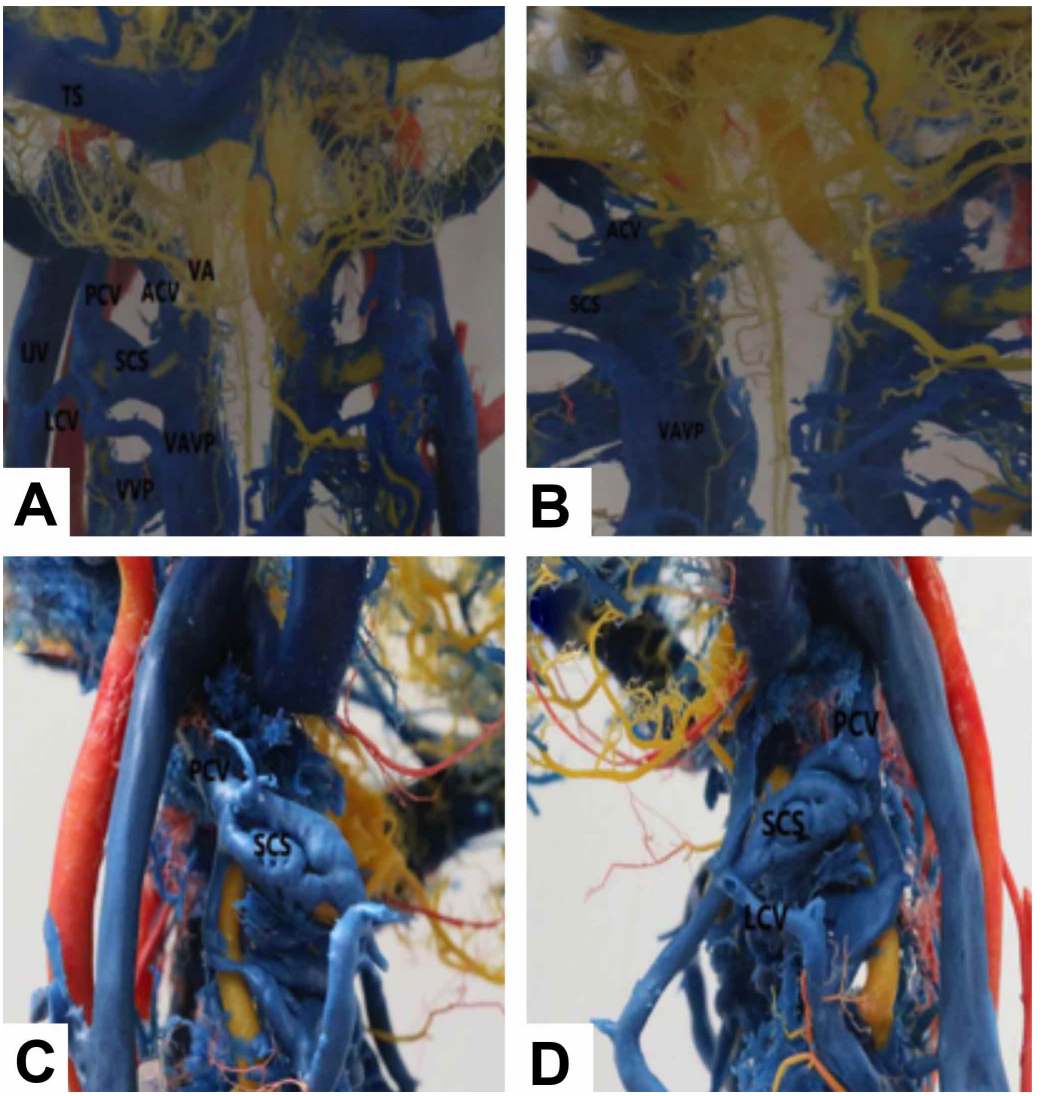

Fig. 3. Suboccipital cavernous sinus (SCS) cast specimens. A: The medial part of SCS communicates superiorly with the anterior condylar vein and inferiorly with the vertebral artery venous plexus. The lateral part of SCS communicates superiorly with the posterior condylar vein and anterolaterally with the vertebral venous plexus through the lateral condylar vein. B: The medial part of SCS extends intracranially through the superior anterior condylar vein and inferiorly with the vertebral artery venous plexus. C: The lateral part of SCS communicates superiorly with the posterior condylar vein. D: The lateral part of SCS communicates superiorly with the posterior condylar vein and anterolaterally with the lateral condylar vein. SCS: suboccipital cavernous sinus; ACV: anterior condylar vein; VAVP: vertebral arterial venous plexus; PCV: posterior condylar vein; LCV: lateral condylar vein; IVJ: internal jugular vein; VA: vertebral artery; TS: transverse sinus; VVP: vertebral venous plexus.

specimens without venous variation, and all vessels were visualised intact (Fig. 3A). The bilateral SCS was displayed intact, which was irregular. It surrounded the venous structure of the horizontal segment (V3) of the vertebral artery and its branches. The medial part of the SCS communicated superiorly with the anterior condylar vein and inferiorly with the venous plexus of the vertebral artery (Fig. 3B). The lateral part of the SCS communicated superiorly with the posterior condylar vein and the sigmoid sinus (Fig. 3C and D) and anterolaterally with the internal vertebral venous plexus through the lateral condylar vein (Fig. 3D).

The MRV imaging results of SCS were consistent with those of the cast specimens. The venous changes were divided into the following three types: Type I: The bilateral presence of posterior condylar and lateral condylar veins; Type II: The unilateral presence of posterior condylar vein; Type III: The unilateral presence of lateral condylar vein (Fig. 4).

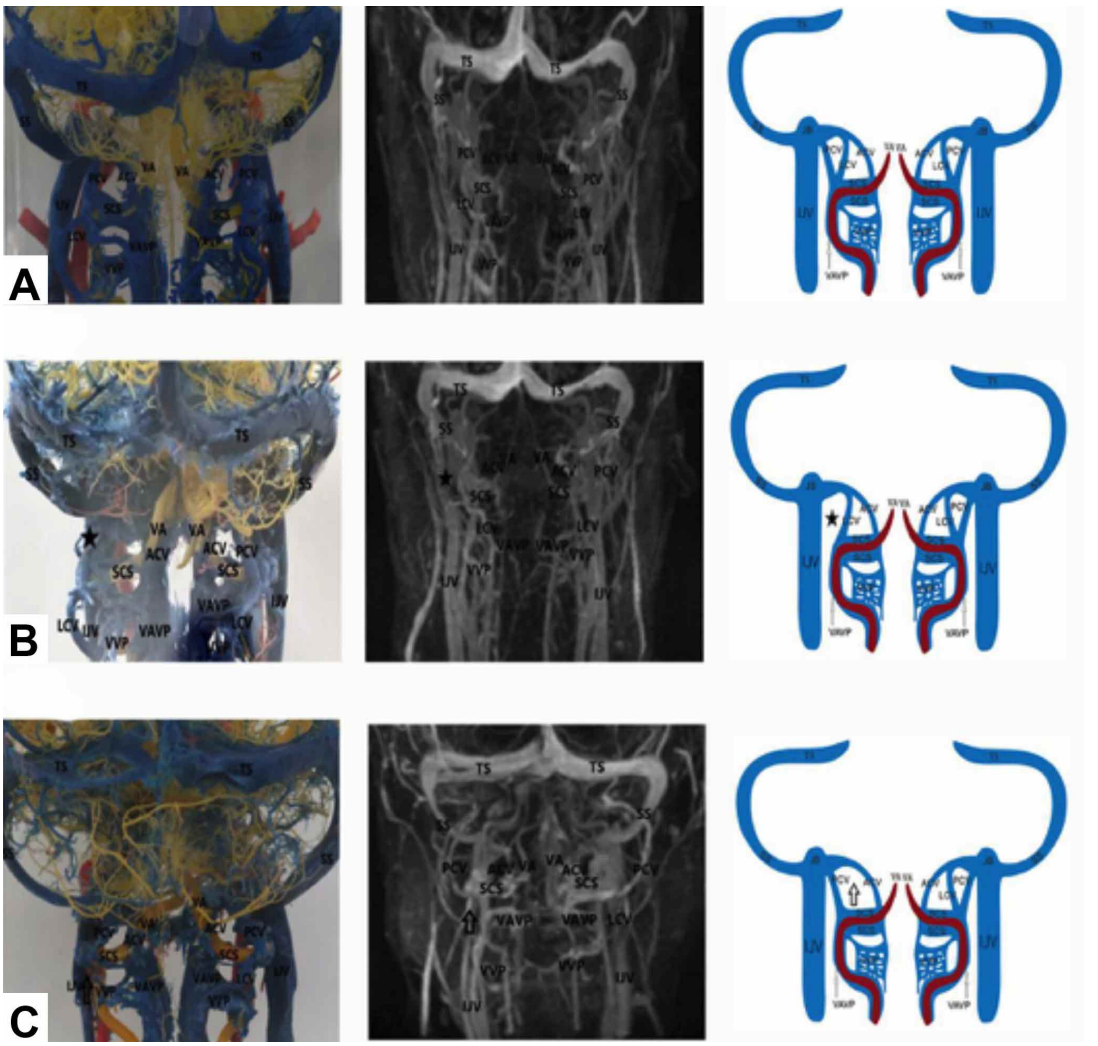

Fig. 4. Comparison between the magnetic resonance venography (MRV) images of the suboccipital cavernous sinus (SCS) and the cast specimens. A. Comparison between the MRV images and the cast specimens. Type I: The bilateral presence of posterior condylar and lateral condylar veins. B. Comparison between the MRV images and the cast specimens. Type II: The unilateral presence of posterior condylar vein (*indicates the unilateral posterior condylar vein (PCV) was not shown). C. Comparison between the MRV images and the cast specimens: Type III: The unilateral presence of lateral condylar vein (⇑ indicates the unilateral lateral condylar vein (LCV) was not shown). SCS: suboccipital cavernous sinus. ACV: anterior condylar vein; VAVP: vertebral arterial venous plexus. PCV. posterior condylar vein. LCV: lateral condylar vein. IVJ: internal jugular vein; VA: vertebral artery; TS: transverse sinus; VVP: vertebral venous piexus; SS: sigmoid sinus.

DISCUSSION

The morphological characteristics and clinical significance of SCS. The CCJ that is located between the skull base and the upper cervical spine contains important structures such as the medulla oblongata, upper cervical spinal cord, cranial nerve, vertebral artery, and internal carotid artery and vein. The SCS that is located at the craniocervical junction is a venous plexus that surrounds the horizontal suboccipital segment (V3) of the vertebral artery and its branches, the periarterial autonomic plexus, and the adjacent spinal nerves (Arnautovic *et al.*, 1997). Surgery is effective for tumours, vascular diseases, and degenerative diseases at the craniocervical junction. The V3 segment of the vertebral artery can directly or indirectly participate in the blood supply and infection of tumours at the craniocervical junction. The V3 itself is also involved in diseases such as a tumour, infections, and malformations,

which can easily result in V3 segment injury during surgery and cause fatal bleeding. Even if the V3 segment is well exposed, opening the posterior atlanto-occipital membrane close to the V3 segment can often cause bleeding in the surrounding SCS (Chen *et al*., 2015; Morota *et al*., 2017). The V3 segment, SCS, and the communicating vascular structures and their adjacency level can help develop a safer surgical approach at the craniocervical junction. This can effectively reduce intraoperative bleeding and postoperative complications.

The MRV imaging technique is mostly used for imaging studies of cranial veins (Fan *et al*., 2021). SCS and communicating vessels can be well displayed in MRV images via direct imaging of the cranial veins. Therefore, the data measurement and image observation of SCS by using MRV are highly precise. SCS displayed a large morphological variation in MRV images, that is, a long strip or oval shape in the coronal and sagittal planes and an irregular sector shape in the transverse plane. Because of the uneven thickness of the transverse SCS, measuring only one diameter will not be standard. Therefore, three positions, namely the initial, middle, and terminal parts, should be selected for the measurement. The measurement plane should be perpendicular to the vertebral artery (Zhao Bibo 2015).

To the best of our knowledge, this study is the first to reconstruct and measure 61 cases of cranial SCS MRV images by using the MRV imaging technique and Mimics19.0 three-dimensional reconstruction technique. The supero-inferior diameter, left-right diameter, anteroposterior diameter of SCS, and distance from the midline and the skin were measured to obtain three-dimensional MRI measurements of the SCS. We observed no significant difference between the left and right sides in each measurement value for the SCS in the transverse, coronal, and sagittal views. However, the diameters of the initial, middle, and terminal parts of the SCS in the transverse view were found to differ significantly, which suggested that SCS was present on both left and right sides of the suboccipital region, with a small two-headed, thick middle structure. Our results have an important reference value for determining the clinically safe surgical range.

Comparison of SCS venous communication between the imaging data and cast specimens. The structural position of SCS and its communicating vessels did not change during fabrication of the cast specimens, which was strictly followed in the present study. We compared the location of SCS and its adjacency with the communicating vessels and found a good corresponding relationship between them. SCS communicated with the anterior condylar vein through its superomedial aspect and the with lateral condylar vein through the anterolateral aspect. SCS communicated with the jugular bulb through the posterior condylar vein and extended inferiorly to the vertebral artery venous plexus. Observation of the cast specimens suggested changes in the posterior condylar vein and lateral condylar vein. The changes in the communicating vessels of the SCS were divided into the following three types: Type I: The bilateral presence of posterior condylar and lateral condylar veins. Type II: The unilateral presence of posterior condylar vein. Type III: The unilateral presence of lateral condylar vein. These variation types well corresponded with those in the MRV images. This observation enriches the anatomical and imaging data of SCS and communicating vessels.

Imaging characteristics of the communicating vessels and clinical significance of the variations in the lateral and posterior condylar veins. The morphology of the anterior, posterior, and lateral condylar veins and marginal sinuses in MRV images showed that these structures were irregular in shape and varied greatly. SCS, marginal sinus, vertebral artery venous plexus, and the anterior condylar vein were visualised. We observed differences in the posterior condylar and lateral condylar veins, which were not seen in 27 % of the posterior condylar vein and 33 % of the lateral condylar vein reported in previous studies (Takahashi *et al*., 2005; Tanoue *et al*., 2010). These changes exhibit great clinical significance. The lateral condylar vein is the main drainage route for some dural arteriovenous fistulas at the CCJ as a venous route during vascular interventions. Neurosurgeons place immense importance to their anatomical variations (Miyachi *et al*., 2008; Matsushima *et al*., 2015). The posterior condylar vein can be considered an intraoperative landmark for performing surgical procedures via the supracondylar or condylar fossa approach (Wen *et al*., 1997; Matsushima *et al*., 2001), and its anatomical variations are of immense importance to surgeons.

Recent studies have reported that in the upright human state, the jugular vein is depressed due to intrathoracic pressure, and the vertebrovenous system becomes the main venous outflow channel in the brain (Epstein *et al*., 1970). The anterior, lateral, and posterior condylar veins are considered important for the communication between the intracranial venous plexus and the vertebral venous plexus. They become important drainage channels for the intracranial veins in the upright human state. Kosugi *et al*. (2020) reported the importance of SCS and communicating vessels in the craniocervical venous communication in the human upright state. This study describes the classification of lateral condylar and posterior condylar vein variations, which not only enriches the fine anatomy of SCS but also facilitates better understanding of the craniocervical blood circulation in the human upright state.

CONCLUSION

The MRV images and cast specimens of the SCS indicated that the SCS has a normal morphological structure and adjacency, thereby providing accurate and complete three-dimensional imaging anatomical data of the SCS and its communicating vascular structures. The findings may help clarify the imaging anatomy relationship between the SCS and its communicating vessels. This study enriches the fine anatomical data of the Chinese SCS and presents morphological reference data for the clinical individualised surgical plan to ensure safety of the surgery.

JIANG, S. M.; LIU, C.; ZHANG, X. H.; ZHENG, N. ; BO YU, S.; CHI, Y. Y.; ZHANG, J. F.; WANG, Y.; SUI, H. J. & XU, Q. Un estudio comparativo de la morfología del seno cavernoso suboccipital utilizando imágenes de resonancia magnética y muestras de yeso. *Int. J. Morphol., 40(4)*:1000-1008, 2022.

RESUMEN: Se realizó un estudio comparativo de la morfología del seno cavernoso suboccipital (SCS) mediante resonancia magnética y muestras de yeso. El presente estudio retrospectivo analizó los datos de imágenes de venografía por resonancia magnética (RNM) craneocervical de 61 pacientes. La reconstrucción tridimensional se realizó con Mimics 19.0. Se midió: el diámetro izquierdo-derecho del SCS (d1), la distancia desde la línea mediana (d2), el diámetro superoinferior (d3), el diámetro anteroposterior (d4), la distancia desde el diámetro posterior hasta la piel (d5) y el diámetro del SCS en diferentes partes (d6-d8). En la comparación entre las imágenes RNM y las muestras de yeso, el SCS, el seno marginal, la vena condilar anterior y el plexo venoso de la arteria vertebral eran simétricos y se observaron bilateralmente, mientras que la presencia de la vena extracondilar y la vena condilar posterior presentaba tipos diferentes. La proximidad del SCS y sus vasos comunicantes y los cambios en sus vasos comunicantes se correspondieron bien con las imágenes de RNM y los especímenes moldeados. Se encontraron muchos tipos de venas condilares laterales y condilares posteriores izquierda y derecha en las muestras de yeso, que podrían dividirse en presencia bilateral de venas condilares posteriores y condilares laterales, presencia unilateral de venas condilares posteriores y presencia unilateral de venas condilares laterales. Un total de 61 casos analizados mediante imágenes MRV revelaron la presencia bilateral de venas condilares posteriores y condilares laterales (77,1 %), la presencia unilateral de venas condilares posteriores (18,0 %) y la presencia unilateral de venas condilares laterales (9,8 %) de los cuales la presencia bilateral de las venas condilar posterior y condilar lateral representó la mayor proporción. Las imágenes de RNM y las muestras de yeso del SCS mostraron su estructura morfológica y adyacencia normales, lo que proporcionó datos anatómicos de imágenes tridimensionales precisos y completos del SCS y sus estructuras vasculares comunicantes. Este estudio enriquece los datos de anatomía de imágenes de SCS chino y puede ser valioso en la práctica clínica.

PALABRAS CLAVE: Seno cavernoso suboccipital; MRV; Espécimen en yeso; Unión craneocervical.

REFERENCES

Arnautovic, K. I.; al-Mefty, O.; Pait, T. G.; Krisht, A. F. & Husain, M. M. The suboccipital cavernous sinus. J. Neurosurg., 86(2):252-62, 1997.

Chen, D.; Chen, W.; Chen, H.; Zhang, X. & Liang, E. Clinical experience of far lateral suboccipital approach for resection of ventral tumors at craniocervical junction. *Chin. J. Neurosurg., 31(3)*:243-5, 2015.

Epstein, H. M.; Linde, H. W.; Crampton, A. R.; Ciric, I. S. & Eckenhoff, J. E. The vertebral venous plexus as a major cerebral venous outflow tract. *Anesthesiology, 32(4)*:332-7, 1970.

Fan, Y.; Li, K.; Wei, L. & Wang, S. Reconstruction of intracranial sickle sinus by MRV imaging anatomy. *Chin. J. Clin. Anat., 39(5)*:529-34, 2021.

Hiramatsu, H.; Sugiura, Y.; Kamio, Y. & Kamiya, M. Transvenous embolization of a dural arteriovenous fistula involving the suboccipital cavernous sinus. *Clin. Neuroradiol., 25(4)*:419-22, 2015.

Kosugi, K.; Yamada, Y.; Yamada, M.; Yokoyama, Y.; Fujiwara, H.; Yoshida, K.; Yoshida, K.; Toda, M. & Jinzaki, M. Posture-induced changes in the vessels of the head and neck: evaluation using conventional supine CT and upright CT. *Sci Rep., 10(1)*:16623, 2020.

Matsushima, K.; Funaki, T.; Komune, N.; Kiyosue, H.; Kawashima, M. & Rhoton Jr., A. L. Microsurgical anatomy of the lateral condylar vein and its clinical significance. *Neurosurgery, 11 Suppl. 2*:135-45; discussion 145-6, 2015.

Matsushima, T.; Matsukado, K.; Natori, Y.; Inamura, T.; Hitotsumatsu, T. & Fukui, M. Surgery on a saccular vertebral artery-posterior inferior cerebellar artery aneurysm via the transcondylar fossa (supracondylar transjugular tubercle) approach or the transcondylar approach: surgical results and indications for using two different lateral skull base approaches. *J. Neurosurg., 95(2)*:268-74, 2001.

Miyachi, S.; Ohshima, T.; Izumi, T.; Kojima, T. & Yoshida, J. Dural arteriovenous fistula at the anterior condylar confluence. *Interv. Neuroradiol., 14(3)*:303-11, 2008.

Morota, N. Pediatric craniovertebral junction surgery. *Neurol. Med. Chir., 57(9)*:435-60, 2017.

Takahashi, S.; Sakuma, I.; Omachi, K.; Otani, T.; Tomura, N.; Watarai, J. & Mizoi, K. Craniocervical junction venous anatomy around the suboccipital cavernous sinus: evaluation by MR imaging. *Eur. Radiol., 15(8)*:1694-700, 2005.

Tanoue, S.; Kiyosue, H.; Sagara, Y.; Hori, Y.; Okahara, M.; Kashiwagi, J. & Mori, H. Venous structures at the craniocervical junction: anatomical variations evaluated by multidetector row CT. *Br. J. Radiol., 83(994)*:831-40, 2010.

Wen, H. T.; Rhoton Jr., A. L.; Katsuta, T. & de Oliveira, E. Microsurgical anatomy of the transcondylar, supracondylar, and paracondylar extensions of the far-lateralapproach. *J. Neurosurg., 87(4)*:555-85, 1997.

Corresponding author:
Dr. Qiang XU
Department of Radiology
The 967 Hospital of the Joint Logistics Support Force
Dalian - CHINA
E-mail: 13332223310@163.com

Corresponding author:
Prof. Hong-Jin Sui
Department of Anatomy
College of Basic Medicine
Dalian Medical University
Dalian - CHINA

E-mail: Suihj@hotmail.com